13

Electrical and optical properties of thin-film bismuth ferrite

© V.A. Dybov, Yu.E. Kalinin, A.A. Kamynin, M.A. Kashirin, V.A. Makagonov, A.E. Nikonov, D.V. Serikov, A.V. Sitnikov

Voronezh State Technical University,
394026 Voronezh, Russia
e-mail: vlad_makagonov@mail.ru

Received July 12, 2022
Revised August 22, 2022
Accepted September 9, 2022

The optical and electrical properties of bismuth ferrite thin films obtained by high-frequency magnetron sputtering in an atmosphere of argon and oxygen (80% + 20%) has been studied. Investigations of the optical properties have shown that for polycrystalline bismuth ferrite films the optical band gap is ~ 2.3 eV, which is in the range of given in the literature values. The dependences of the specific electrical conductivity on the magnitude of the electric field has been studied for the synthesized films. It has been established that the electrical conductivity does not depend on the electric field strength up to the value of $E = 2.1 \cdot 10^6$ V/m. The experimental results are discussed in terms of the model of charge carrier injection from aluminum electrode into the conduction band of bismuth ferrite.

Keywords: electrical conductivity, strong electric fields, optical absorption coefficient, memristor effect.

DOI: 10.21883/TP.2022.12.55208.182-22

Introduction

The use of semiconductor and dielectric materials based on metal oxides for the needs of optoelectronics, power electronics, spintronics and many other areas is more and more considered in modern fundamental and applied studies [1]. Interest in these materials is due to their properties such as thermal stability at high temperatures, optical transparency, the ability to control electrical and magnetic properties, etc. [2]. Thin-film coatings of metal oxides are an extensive group of the most demanded materials in modern micro- and nanoelectronics [3]. In particular, thin films of bismuth ferrite are considered, which, due to its electrical, optical, gas-sensitive and other properties, belongs to one of the popular multiferroics with the perovskite structure [4,5]. Crystalline bismuth ferrite $BiFeO_3$ has high temperatures of ferroelectric ($T_c = 1083$ K) [6] and magnetic ($T_N = 673$ K) [7] ordering, i. e. has a sequence of phase transitions accompanied by magnetoelectric interactions [8]. The increased interest in bismuth ferrite in world science is due, among other things, to the prospects for its application in spintronics, sensor technology, and microwave electronics [9,10].

Most studies of the structure and physical properties of bismuth ferrite thin films were carried out on polycrystalline and epitaxial structures. In particular, it was found in the paper [11] that bismuth ferrite films with (111) orientation grow epitaxially on (111) $SrTiO_3$ substrates. In paper [12] thin films of bismuth ferrite were deposited on $Pt/Ti/SiO_2/Si(100)$ substrates at deposition temperatures of 350, 400 and 450°C respectively. The deposition process was carried out in a high-frequency magnetron sputtering system, and $Bi_{1.1}FeO_3$ ceramics was used as a target. During deposition, a gas mixture of $Ar/O_2 = 4:1$ was introduced at a common pressure, and the input power was maintained at level of 80 W.

The studies performed shown that the sequence of phase transitions in epitaxial bismuth ferrite films, as well as the temperature regions of the coexistence of magnetic and polarization orders can differ significantly from those observed in bulk materials. Bismuth ferrite epitaxial films were synthesized on various substrates and buffer layers, and, in addition to the rhombohedral phase, very diverse structural distortions were found that are not observed in bulk bismuth ferrite: tetragonal, orthorhombic, monoclinic, and triclinic [13].

Many physical properties of oxide materials in general, and electrical resistivity in particular are determined by the presence of oxygen vacancies in them, which finds application in structures called memristors [14]. One of the promising types of memristors, the switching mechanism of which is presumably related to the drift of oxygen vacancies, includes memristors based on oxides with a high permittivity, since the activation energy of the hopping transfer of oxygen vacancies E_m in them is relatively low. For example, in the case of amorphous bismuth ferrite the value $E_m \approx 0.8$ eV [15]; for comparison in Al_2O_3 value $E_m \approx 6$ eV [16,17]. The resistive switching mechanism was studied in relative detail in metal–dielectric–metal (MDM) structures based on crystalline $LiNbO_3$ [18], in which a small activation energy $E_m \approx 0.67$ eV [19] is observed.

On the other hand, in oxide semiconductors with amorphous structure and high electrical resistivity, the concentration of free carriers is extremely low, and their electrical transfer is determined by the presence of traps in the forbidden band, and donors located deep in it. The

properties of donors fundamentally differ from those of traps, since traps do not have their own electrons, but only capture electrons injected from contacts. Donors have their own electrons [20]. In 1938 Frenkel proposed a theoretical substantiation of the exponential dependence of the current on the electric field for semiconductors with traps [21].

In view of the foregoing, in this paper the goal is to study the structure, width of forbidden band, and electrical resistivity of thin films of bismuth ferrite, to investigate the effect of a strong electric field on the electrical conductivity in the amorphous state, and to study the possibility of observing the memristor effect in two-layer structures based on amorphous bismuth ferrite with different oxygen concentrations in layers.

1. Sampling and experiment procedure

To obtain thin-film samples of bismuth ferrite, the method of high-frequency magnetron sputtering (HFMS) [22] was used. The HFMS method was carried out on unit created on the basis of industrial vacuum sputtering station UVN-74, upgraded with a planar magnetron with a cathode size of 70×300 mm, and with the ability to change the magnetic system dimensions from 45×45 to 45×250 mm. To supply alternating voltage to the cathode of the magnetron, a UV−1 generator unit of high frequency 13.56 MHz and a matching unit were installed. The maximum power of the RF generator — 1000 W. To supply voltage to the cathode of the ion source, a power supply unit of the BP−94 type was installed.

The working gas of the magnetron — argon (99.998%) and oxygen (99.98%). In the course of operation a continuous change of the working gas in the chamber took place due to the inlet through the metering valve and pumping out with a diffusion pump. The vacuum chamber was preliminarily evacuated to a pressure maximum $1 \cdot 10^{-3}$ Pa. During the magnetron operation the following sputtering modes were used: argon pressure in the chamber $1 \cdot 10^{-1}$ Pa, specific power of the HF discharge 50 W. $BiFeO_3$ ceramics was used as a target. Thin films of bismuth ferrite were obtained by high-frequency magnetron sputtering of a ceramic target in Ar (80%) + O_2 (20%) medium. During the deposition process a continuous flow of argon and oxygen was supplied to the chamber, and their flow rate was controlled in the ratio 4 : 1. The substrate was not heated during the deposition process. The substrate temperature was monitored by a chromel−alumel thermocouple, and its value did not exceed 150°C. As substrates the oxidized single-crystal silicon wafers 150 μm thick (oxide thickness 200 nm) to study the structure and electrical properties were used, as well as glass slides to study the optical properties. The thickness of the obtained films was measured on MII-4 interferometer and was 500 nm for samples on silicon and 1 μm for samples on glass. Heat treatment of amorphous films was carried out in a muffle furnace in air at 550°C. The heating and cooling rate was 5 degrees per minute, the holding time at the annealing temperature was 60 min.

The obtained samples were certified using X-ray diffraction analysis (XDA) with the help of Bruker D2 Phaser X-ray diffractometer.

To study the effect of a strong electric field on the conductivity of thin films of bismuth ferrite and memristor structures based on them the structures were synthesized that are MDM structures with aluminum contacts 0.4×0.2 mm.

When measuring the electrical properties of the synthesized structures in strong electric fields, an automated unit based on a MOTECH programmable power supply was used. The process of measurement and experimental data acquisition was carried out automatically using software developed involving LabVIEW environment [23].

To study the optical properties and characteristics of the band structure of oxide semiconductors and structures based on them, the optical measurement methods are actively used. The most common type of optical research is the optical transmittance measurement. Measurements of thin-film bismuth ferrite samples obtained on glass substrates were carried out using ECOVIEW UV-6100C spectrophotometer designed to study the optical transmittance of liquid and solid samples in the ultraviolet, visible, and near-infrared spectral ranges. The optical scheme is two-beam with a bandwidth of 1.8 nm. Spectral measurement range is 190−1100 nm. The measurement range of the optical transmittance is 0.1−100.0%. The measurement error of optical values is $\pm 0.3\% T$ (T — optical transmission). The repeatability of optical measurements is within — 0.2%.

2. Experimental results and discussion

2.1. Structure of bismuth ferrite thin films

Fig. 1 shows the results of X-ray diffraction of synthesized bismuth ferrite films on silicon. In the initial state the synthesized sample has X-ray amorphous structure, which is expressed in the presence of a wide halo at an angle of $2\Theta \approx 29^\circ$ (curve *1* in Fig. 1).

After heat treatment in air at 550°C, the bismuth ferrite film crystallizes, and a series of diffraction maxima is observed in the diffraction pattern (curve *2* in Fig. 1). The analysis of the obtained X-ray diffraction pattern showed that the high-intensity reflections present on it and correspond to the rhombohedral $BiFeO_3$ phase with cell parameters $a = 5.552$ Å, $c = 13.805$ Å. The size of $BiFeO_3$ crystallites, obtained on the basis of estimates by the Scherer method, was 127 nm. There is also a certain amount of the secondary phase $Bi_2Fe_4O_9$, the content of which in the film does not exceed 2%. The presence of this phase is due to the instability of the $BiFeO_3$ phase both during synthesis, and during subsequent heat treatment [24,25].

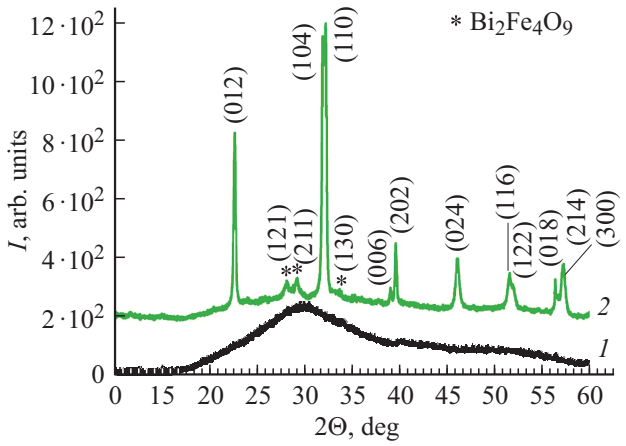

Figure 1. X-ray patterns of a $BiFeO_3$ film on a silicon substrate in the initial state (curve *1*) and after heat treatment in air at 550°C for 60 min (curve *2*). The sign ⟨∗⟩ denotes the $Bi_2Fe_4O_9$ impurity phase.

2.2. Optical properties of bismuth ferrite thin films

To study the optical properties and determine the forbidden band width of the bismuth ferrite thin films, the light transmission spectra were measured on samples de[osited on glass substrates. The measurements were carried out in the wavelength range from 300 to 1100 nm at room temperature.

The optical transmission spectra of the films studied in this paper are shown in Fig. 2. As can be seen from the Figure, the resulting films are transparent in the wavelength range from 550 to 1100 nm. A sharp decrease in transmission in the region of wavelengths less than 550 nm is associated with fundamental absorption.

In the general case, the fundamental absorption edge can be described by the Tauc formula [26]:

$$\alpha h\nu = a \cdot (h\nu - E_g)^n, \qquad (1)$$

where $\alpha = -\ln T/d$ — absorption coefficient (T — optical transmission, d — film thickness), $h\nu$ — energy photons, E_g — optical band gap, A — constant depending on the effective masses of electrons in the conduction band and holes in the valence band, n — determines the type of electron or optical transition and takes the values 1/2, 2, 3/2 or 3. If $n = 1/2$, then the transition is a direct allowed, $n = 3/2$ — a direct forbidden, $n = 2$ — an indirect allowed, and for $n = 3$ — indirect forbidden [26]. Usually the contribution of allowed transitions dominates in absorption processes, giving either $n = 1/2$ for direct transitions or $n = 2$ for indirect transitions.

To establish the optical width of the forbidden band of the studied films, the experimental optical transmission spectra were rearranged in the coordinates $\alpha^2 = h\nu$, $\alpha^{1/2} = h\nu$, and it was found that the studied thin films belong to direct-band semiconductors. From the spectral dependence of the absorption coefficient, which satisfies a direct-band semiconductor, linear extrapolation of the dependence $(\alpha h\nu)^2$ from the photon energy $h\nu$ to the value $\alpha = 0$ in the region of the fundamental absorption edge determined the optical width of forbidden band E_g^{opt} (Fig. 3). Estimates shown that for bismuth ferrite films obtained in argon and oxygen atmosphere in the initial state, the optical width of the forbidden band is about 2.7 eV, and after heat treatment in air at 550°C for 60 min — about 2.3 eV, which is in the range of values given in the literature for oxide perovskites based on $BiFeO_3$ [27,28].

To calculate the average (in the studied wavelength range) value of the refractive index n, we use the formula that follows from the condition for interference observation under the condition of normal incidence of light [29,30]:

$$n = \frac{m}{2d\left(\frac{1}{\lambda_1} - \frac{1}{\lambda_2}\right)}, \qquad (2)$$

where d — thickness of the film under study, λ_1 and λ_2 — wavelengths corresponding to the chosen maxima,

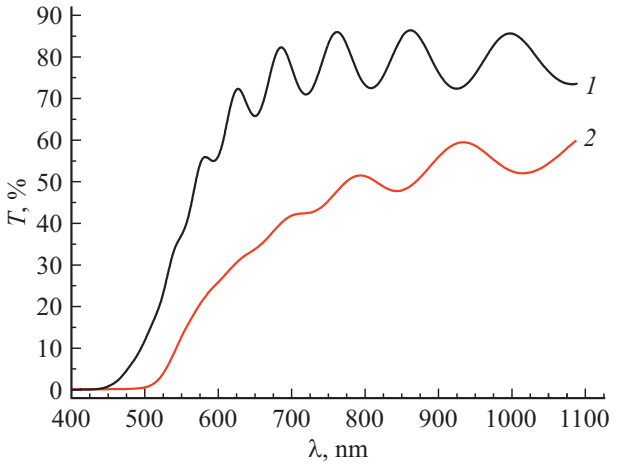

Figure 2. Optical transmission spectra of bismuth ferrite film with thickness of 1 μm in the initial state (*1*) and after heat treatment at $T = 550$°C for 60 min (*2*).

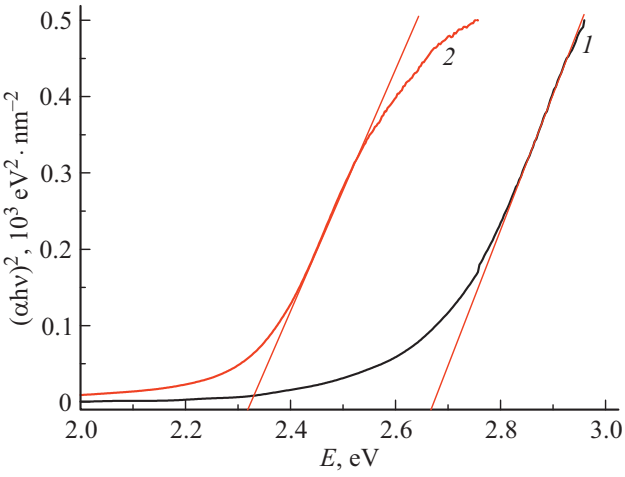

Figure 3. Optical absorption coefficient α vs. energy of incident photons E, presented in the coordinates $(\alpha h\nu)^2 \propto E$ and measured for bismuth ferrite films 1 μm thick in the initial state (*1*) and after heat treatment at $T = 550$°C for 60 min (*2*).

m — integer number provided that two adjacent maxima are taken. Estimates of the average optical refractive index gave the values $n = 3.22$ for films in the amorphous state and $n = 2.64$ for bismuth ferrite films after heat treatment. Note that the obtained values of n are in the range of values given in the literature for polycrystalline thin films of $BiFeO_3$ [31,32].

2.3. Influence of strong electric field on conductivity of the bismuth ferrite thin films

2.3.1. Conductivity of bismuth ferrite thin film in strong fields

Preliminary results of electrical properties study of bismuth ferrite thin films showed that the latter have a high electrical resistance; therefore, thin film samples were synthesized for studies in perpendicular geometry, and the effect of strong electric field on their conductivity was studied. Fig. 4 shows the current-voltage characteristics (CVC) of the investigated bismuth ferrite 500 nm thick.

CVC of films of bismuth ferrite thin film is symmetric with respect to zero and non-linear. The dependences measured at the increase and decrease in the electric field are the same. To analyze the obtained dependences, the positive branch of the CVC (the first quadrant) was chosen, from which the electrical conductivity values were calculated. The conductivity vs. electric field strength of the studied films shown on Fig. 5 can be conditionally divided into two portions.

The first section I corresponds to a linear change in the current with increase in the electric field strength up to the values of $E = 2.1 \cdot 10^6$ V/m — ohmic section, on which the electrical conductivity does not depend on the electric field strength. The specific electrical conductivity determined from the ohmic conductivity section was $5.8\,\mu\Omega^{-1} \cdot \mathrm{m}^{-1}$. The second section II is characterized by a pronounced nonlinear dependence of the electrical conductivity on the field, and the conductivity begins to increase nonlinearly at $E > 2.1 \cdot 10^6$ V/m.

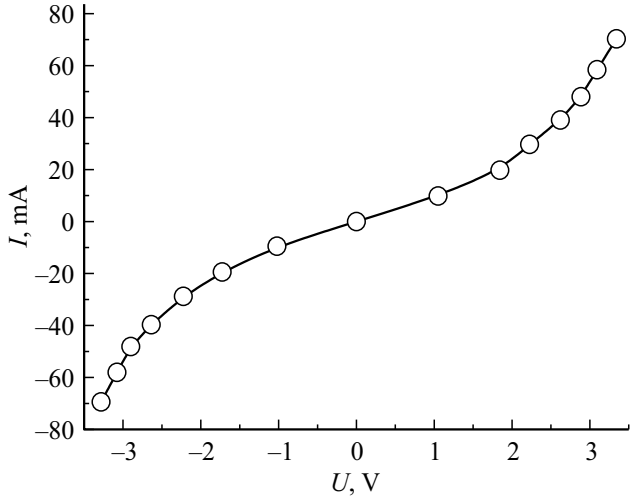

Figure 4. CVC of bismuth ferrite thin film 500 nm thick in the initial state.

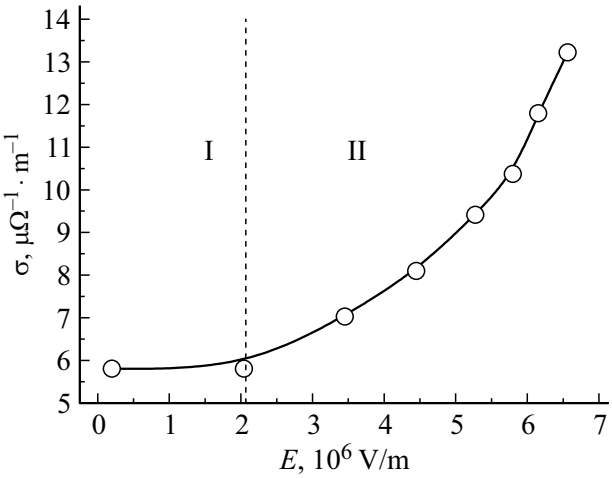

Figure 5. Electrical conductivity vs. strength of external electric field of bismuth ferrite thin film in the initial state.

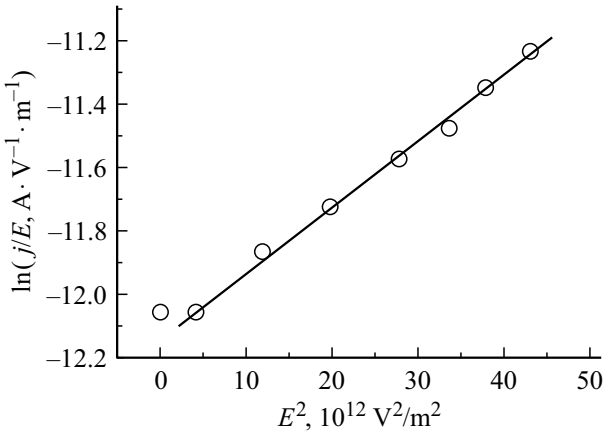

Figure 6. CVC of bismuth ferrite thin film, rearranged in coordinates corresponding to the model of injection of charge carriers from aluminum into bismuth ferrite by the mechanism of thermally facilitated tunneling.

In limit cases the conductivity can be limited by the carriers injection at the contact or by transfer through traps in the bulk. Such a division is often conditional, depending on how strongly the space charge accumulated on the traps shields the electric field on the contact. In this case, oxygen vacancies act as traps, which in the initial state are not filled with electrons and holes. The analysis of the effect of the electric field strength on the conductivity of bismuth ferrite thin film during transfer limited by the volume of the dielectric was carried out according to the models of trap ionization according to Frenkel [21] and hopping electrical conductivity through traps under conditions of strong electric field [33]. The analysis showed that the experimental results cannot be well described within the framework of any of the indicated models of transfer over the bulk of the dielectric.

Three injection mechanisms are usually considered on the contact: the Fowler–Nordheim effect, thermally facilitated tunneling, and Schottky thermionic emission [20]. To analyze the experimental results in terms of their correspondence to these supposed mechanisms, the CVC of the studied samples presented in Fig. 4 were rearranged in coordinates corresponding to the Fowler–Nordheim mechanisms $\ln(j/E^2) \propto f(1/E)$, thermally facilitated tunneling $\ln(j/E) \propto f(E^2)$ and the Schottky effect $\ln(j) \propto f(\sqrt{E})$, where j — current density. For bismuth ferrite films we obtain the best linearization of the experimental curve in coordinates corresponding to the mechanism of thermally facilitated tunneling (Fig. 6).

For bismuth ferrite films at an electric field strength from $E = 2.1 \cdot 10^6$ to $6.6 \cdot 10^6$ V/m, the linear section on the experimental curves in the coordinates $\ln(j/E) \propto E^2$ indicates the prevailing role of the thermally facilitated tunneling mechanism in the electrical transfer of the studied samples.

Thus, in the synthesized bismuth ferrite thin films the conductivity in the region of strong electric fields is determined by the injection of charge carriers from the contact into the bulk and by charge transfer in the bulk of the film.

2.3.2. Memristor properties of structures based on bismuth ferrite thin film

Most often the memristor cell based on a metal oxide is an MDM structure in which a stoichiometry gradient with respect to oxygen is created in the dielectric material [34]. To obtain the gradient of oxygen content through the thickness of the dielectric layer, the sequential deposition was carried out in argon medium (11 min, $P_{\mathrm{Ar}} = 1.2$ Pa) and medium $\mathrm{Ar} + \mathrm{O_2}$ (22 min, $P_{\mathrm{Ar+O_2}} = 1.2$ Pa) at a magnetron power of 50 W. Thus, the thickness of the $BiFeO_3$ layer depleted in oxygen was 20 nm, and the thickness of the enriched layer was 40 nm. The dimensions of the aluminum contacts, as in the study of the strong field effect on the electrical conductivity of the bismuth ferrite thin film, was $0.4 \times 0.2\,\mathrm{mm}^2$.

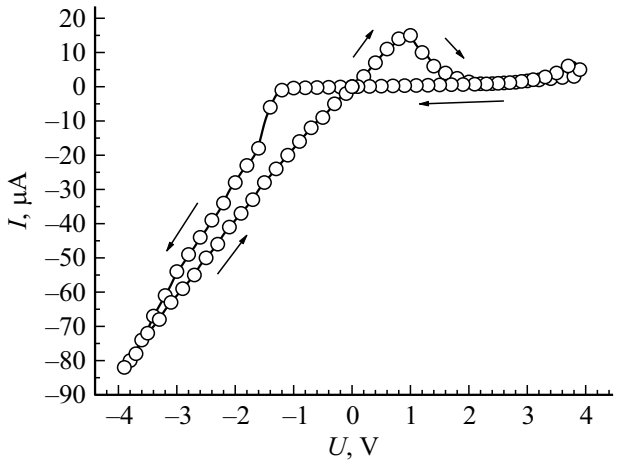

Figure 7. CVC of synthesized two-layer structure based on bismuth ferrite 60 nm thick at room temperature.

Fig. 7 shows CVC of synthesized structure based on bismuth ferrite at room temperature. It can be seen from the above dependence that at voltage $\sim -(2-4)$ V the current through the structure sharply increases, which corresponds to decrease in the electrical resistance of the sample, i.e. transition to the „low-resistance“ state (LRS). As the voltage decreases from -4 to $+1$ V, the CVC of the structure is practically linear, which indicates the constant electrical resistance of the film. At voltage greater than $+1$ V the electric current through the film decreases sharply, which indicates increase in the electrical resistance of the sample and the structure switching into the „high-resistance“ state (HRS).

Estimates of the resistance of the resulting structure at voltage of $+0.2$ V (readout voltage) give the values $\approx 67\,\mathrm{k\Omega}$ for the LRS state and $\approx 3\,\mathrm{M\Omega}$ for the HRS state. Thus, during the transition from the LRS to the HRS state and vice versa the resistance of the resulting structure changes by a little less than 50 times. The considered example of the formed CVC shows that the synthesized structure based on bismuth ferrite can have good memristor properties.

Let's discuss the results. To date, rather rich experimental material was accumulated, which contains, among other things, the evidence base for the key role of oxygen vacancies (ions) in the resistive switching of many objects based on metal oxides. In this case, in almost all cases it is noted that switching occurs when the critical field ($\sim 10^5\,\mathrm{V \cdot cm^{-1}}$) is reached in very short time. One of the possible switching mechanisms is the formation of a conducting channel, which provides a low-resistance state of the memristor [35]. However, different opinions arise regarding the formation mechanism of the conducting channel itself: some authors associate the switching with a purely thermal effect [36,37], others — with electronic process similar to the double injection process [38].

For the studied structure, this process can be associated with electronic process, in which strong electric field is formed between the electrodes in two-layer bismuth ferrite. As shown in the previous section, in the single-layer structure of bismuth ferrite, the process of thermally facilitated tunneling on the contact prevails, when at the first stage charge carriers (electrons) are excited to a certain energy due to the phonons absorption, at the second stage they tunnel into the free band of bismuth ferrite. In this case, the process of charge transfer in two-layer structure with different concentration of traps (oxygen vacancies) will depend on the polarity of the applied electric field. If a negative potential is applied to the upper electrode located on a layer of bismuth ferrite, which is synthesized in the argon atmosphere and contains a higher concentration of oxygen vacancies, then charge carriers can be injected into the high-resistance layer through traps contained in the low-resistance layer. The formation of conducting channels in the lower (high-resistance) layer, which was synthesized in argon + oxygen atmosphere and contains

lower concentration of oxygen vacancies is reflected by the negative branch of CVC (Fig. 7).

If, however, a positive potential is applied to the upper electrode, then at low electric field strengths the conductivity will be due to the charge carriers located in the traps. When the critical value corresponding to the transition to the strong field is reached, the charge carriers are already injected at the lower electrode due to thermally facilitated tunneling, which conduct electric current through the traps. In this case, due to the application of the strong electric field, negatively charged oxygen ions receive a directed drift to the positive electrode, begin to accumulate on it, creating a space charge that screens the electric field on the contact. This process is accompanied by a sharp drop in the electric current and is reflected by the positive branch of the CVC (Fig. 7).

Finally note that memristors operating based on the switching mechanism proposed in this paper should have more reproducible parameters than memristors, in which the switching process is based on the formation of filaments from oxygen vacancies, through which charge transfer occurs [39].

Consequently, the switching processes in the studied structures of bismuth ferrite can be associated with the processes of charge carrier injection into the high-resistance layer through traps contained in the low-resistance layer (at a negative potential at the electrode) and the formation of space charge screening the electric field at the contact (at a positive potential). Further studies of the memristive properties in the structures studied in this Section and on other oxides will make it possible to establish more detail mechanism of resistive switching in memristors of this type.

Conclusion

1. Bismuth ferrite thin films 500 nm thick on oxidized silicon substrates and 1 μm thick on glass substrates were synthesized by the HFMS method. The bismuth ferrite films obtained in this paper have the amorphous structure and crystallize at temperature of 550°C. Studies of the optical properties of the synthesized films shown that for bismuth ferrite films in the initial state the optical width of the forbidden band is about 2.7 eV, and for those heat-treated in air at 550°C for 60 min — about 2.3 eV, which is in the range of values given in the literature for perovskite oxides.

2. CVC of the synthesized films were studied, and it was found that the electrical conductivity does not depend on the electric field strength up to the value $E = 2.1 \cdot 10^6$ V/m, is determined by the injection of charge carriers from the contact into the bulk and the charge transfer in the bulk of the material.

3. It has been established that CVC of two-layer MDM structures consisting of oxygen-depleted and oxygen-enriched layers 20 and 40 nm thick, respectively, are characterized by nonlinearity and hysteresis characteristic for the resistive switching effect. During the transition from the LRS to the HRS state and vice versa the resistance of the resulting structure changes by a little less than 50 times. The switching processes in the studied structures are associated with the charge carrier injection into the high-resistance layer through traps contained in the low-resistance layer (at a negative potential at the electrode) and the formation of space charge screening the electric field at the contact at a positive potential.

Funding

The study was supported by the Ministry of Science and Higher Education of the Russian Federation (project № FZGM-2020-007) and the Ministry of Science and Higher Education of the Russian Federation under the project under the agreement № 075-15-2021-709, unique project identifier RF -2296.61321X0037 (control measurements execution).

Conflict of interest

The authors declare that they have no conflict of interest.

References

[1] G.J. Exarhos, X.D. Zhou. Thin Solid Films, **515** (18), 7025 (2007). DOI: 10.1016/j.tsf.2007.03.014
[2] E. Fortunato, D. Ginley, H. Hosono, D.C. Paine. MRS Bulletin, **32** (3), 242 (2007). DOI: 10.1557/mrs2007.29
[3] S.J. Lee, C.S. Hwang, J.E. Pi, J.H. Yang, C.W. Byun, H.Y. Chu, K.I. Cho, S.H. Cho. Etri J., **37** (6), 1135 (2015). DOI: 10.4218/etrij.15.0114.0743
[4] M.D. Rossell, R. Erni, M.P. Prange, J.C. Idrobo, W. Luo, R.J. Zeches, S.T. Pantelides, R. Ramesh. Phys. Rev. Lett., **108** (4), 047601 (2012). DOI: 10.1103/PhysRevLett.108.047601
[5] O.B. Romanova, V.V. Kretinin, S.S. Aplesnin, M.N. Sitnikov, L.V. Udod, K.I. Yanushkevich. Phys. Solid State, **63** (6), 897 (2021). DOI: 10.1134/S1063783421060184
[6] J.R. Teague, R. Gerson, W.J. James. Solid State Commun., **8** (13), 1073 (1970). DOI: 10.1016/0038-1098(70)90262-0
[7] Y.H. Chu, L.W. Martin, M.B. Holcomb, M. Gajek, S. Han, Q. He, N. Balke, C.-H. Yang, D. Lee, W. Hu, Q. Zhan, P.-L. Yang, A. Fraile-Rodríguez, A. Scholl, S.X. Wang, R. Ramesh. Nature Mater., **7**, 478 (2008). DOI: 10.1038/nmat2184
[8] P. Fischer, M. Polomska, I. Sosnowska, M. Szymanski. J. Phys C: Solid State Phys., **13** (10), 1931 (1980). DOI: 10.1088/0022-3719/13/10/012
[9] F. Scott. J. Mater. Chem., **22**, 4567 (2012). DOI: 10.1039/C2JM16137K
[10] A.P. Pyatakov, A.K. Zvezdin. Phys.-Usp., **55** (6), 557 (2012). DOI: 10.3367/UFNe.0182.201206b.0593
[11] J.F. Li, J.L. Wang, M. Wuttig, R. Ramesh, N. Wang, B. Ruette, A.P. Pyatakov, A.K. Zvezdin, D. Viehland. Appl. Phys. Lett., **84** (25), 5261 (2004). DOI: 10.1063/1.1764944
[12] S.R. Jian, H.W. Chang, Y.C. Tseng, P.H. Chen, J.Y. Juang. Nanoscale Res. Lett., **8**, 297 (2013). DOI: 10.1186/1556-276X-8-297

[13] D. Sando, A. Barthélémy, M. Bibes. J. Phys.: Condens. Matter., **26** (47), 473201 (2014). DOI: 10.1088/0953-8984/26/47/473201
[14] *Resistive Switching: From Fundamentals of Nanoionic Redox Processes to Memristive Device Applications*. ed. by D. Ielmini, R. Waser (Wiley-VCH Verlag GmbH & Co. KGaA, Weinheim, Germany, 2016)
[15] S.A. Gridnev, Yu.E. Kalinin, V.A. Dybov, I.I. Popov, M.A. Kashirin, N.A. Tolstykh. J. Alloys Compd., **918**, 165610 (2022). DOI: 10.1016/j.jallcom.2022.165610
[16] R.A. De Souza, V. Metlenko, D. Park, T.E. Weirich. Phys. Rev. B, **85** (17), 174109 (2012). DOI: 10.1103/PhysRevB.85.174109
[17] J.D. Cawley, W. John, A.R. Cooper. J. Am. Ceram. Soc., **74** (9), 2086 (1991). DOI: 10.1111/j.1151-2916.1991.tb08264.x
[18] X. Pan, Y. Shuai, C. Wu, W. Luo, X. Sun, H. Zeng, S. Zhou, R. Böttger, X. Ou, T. Mikolajick, W. Zhang, H. Schmidt. Appl. Phys. Lett., **108** (3), 032904 (2016). DOI: 10.1063/1.4940372
[19] C. Wang, J. Sun, W. Ni, B. Yue, F. Hong, H. Liu, Z. Cheng. J. Am. Ceram. Soc., **102** (11), 6705 (2019). DOI: 10.1111/jace.16522
[20] K.A. Nasyrov, V.A. Gritsenko. Phys.-Usp., **56** (10) 999 (2013).
[21] J.I. Frenkel. Phys. Rev., **54**, 647 (1938). DOI: 10.1103/PhysRev.54.647
[22] M. Sumets, V. Ievlev, V. Dybov, A. Kostyuchenko, D. Serikov, S. Kannykin, E. Belonogov. J. Mater. Sci. Mater. Electron., **30** (17), 16562 (2019). DOI: 10.1007/s10854-019-02033-1
[23] Yu.E. Kalinin, A.V. Sitnikov, V.V. Rylkov, K.G. Korolev, G.S. Ryzhkova. Vestnik VGTU, **12** (6), 4 (2016). (in Russian)
[24] S.M. Selbach, M.A. Einarsrud, T. Grande. Chem. Mater., **21** (1), 169 (2009). DOI: 10.1021/cm802607p
[25] N. Wang, X. Luo, L. Han, Z. Zhang, R. Zhang, H. Olin, Y. Yang. Nano-Micro Lett., **12**, 81 (2020). DOI: 10.1007/s40820-020-00420-6
[26] B.D. Viezbicke, S. Patel, B.E. Davis, D.P. Birnie. Phys. Stat. Sol. B, **252**, 1700 (2015). DOI: 10.1002/pssb.201552007
[27] D. Sando, C. Carrétéro, M.N. Grisolia, A Barthélémy, V. Nagarajan, M. Bibes. Adv. Opt. Mater., **6** (2), 1700836 (2017). DOI: 10.1002/adom.201700836
[28] P. Machado, I. Cañ o, C. Menéndez, C. Cazorla, H. Tan, I. Fina, M. Campoy-Quiles, C. Escudero, M. Tallarida, M. Coll. J. Mater. Chem. C, **9** (1), 330 (2021). DOI: 10.1039/d0tc04304d
[29] F. Carreñ o, J.C. MartínezAntón, E. Bernabeu. Rev. Sci. Instrum., **65** (8), 2489 (1994). DOI: 10.1063/1.1144707
[30] A.R. Ansari, A.H. Hammad, M.Sh. Abdel-wahab, M. Shariq, M. Imran. Opt. Quant. Electron., **52**, 426 (2020). DOI: 10.1007/s11082-020-02535-x
[31] D.J. Huang, H.M. Deng, F. Chen, H. Deng, P.X. Yang, J.H. Chu. J. Phys.: Conf. Ser., **276**, 012168 (2011). DOI: 10.1088/1742-6596/276/1/012168
[32] H. Shima, H. Naganuma, S. Okamura. in *Materials Science — Advanced Topics* (IntechOpen London, United Kingdom, 2013), DOI: 10.5772/54908DOI: 10.5772/54908 p. 33
[33] N. Mott, E. Davis *Electronic Processes in Non-Crystalline Materials* (Clarendon Press, Oxford, 1979)
[34] D.B. Strukov, G.S. Snider, D.R. Stewart, R.S. Williams. Nature, **53**, 80 (2008). DOI: 10.1038/nature06932
[35] D.H. Kwon, K.M. Kim, J.H. Jang, J.M. Jeon, M.H. Lee, G.H. Kim, X.S. Li, G.S. Park, B. Lee, S. Han, M. Kim, C.S. Hwang. Nat. Nanotechnol., **5** (2), 148, (2010). DOI: 10.1038/nnano.2009.456
[36] W. Zhang, R. Mazzarello, M. Wuttig, E. Ma. Nat. Rev. Mater., **4**, 150 (2019). DOI: 10.1038/s41578-018-0076-x
[37] N.A. Bogoslovskiy, K.D. Tsendin. Semiconductors, **46** (5), 559 (2012). DOI: 10.1134/S1063782612050065
[38] L.O. Chua. IEEE Trans. Crcuits Syst. I Regul. Pap., **18** (5), 507 (1971). DOI: 10.1109/TCT.1971.1083337
[39] A. Mehonic, A.L. Shluger, D. Gao, I. Valov, E. Miranda, D. Ielmini, A. Bricalli, E. Ambrosi, C. Li, J.J. Yang, Q. Xia, A.J. Kenyon. Adv. Mater., **30** (43), 1801187 (2018). DOI: 10.1002/adma.201801187